Analytical Investigation On The Performance Of Laminar To Turbulent Transition Over A Wing

Amir Zare Shahneh
Lecturer, Centre of Aeronautics, Cranfield University, UK

Alasdair MacBean
Researcher, Centre of Aeronautics, Cranfield Univesity, UK

***Abstract*—Increasing the extent of laminar flow region over an aircraft wing suggests a lower friction drag which also contributes fuel tank capacity drawback. A balance between these can benefit the design of new wings for aircraft. Among of passive and active methods are used in air flow treatment, hybrid laminar flow control system, which sucks air from the boundary layer into the leading edge of a wing to suppress airflow instabilities and delay transition to turbulent flow, is the purely analytical work presented here for the purpose of reducing drag and making the aircraft more efficient. This study introduces Laminar Flow Control systems and by employing the fundamental equations required, to achieve the required levels of suction across a wing to efficiently suppress flow. A novel system was designed that could be incorporated into the leading edge of large civil aircraft or adapted to suit alternative aircraft using a combination of active and passive suction methods. The active system uses electric or bleeds air to provide the required levels of suction, whereas the passive system automatically produces suction by introducing ducting from the high pressure region at the leading edge to the low pressure region at the underside of the wing. This method reduced the overall power requirement of the active system. Analysis of the design, including the impact of the system weight and fuel penalties found that the system could save over 5.5% of fuel during long-range flights, equivalent to up to 4,000 N of additional payload.**

Keywords—Laminar, Turbulent, CFD, Passive method, Aircraft, Hybrid, Suction

I. INTRODUCTION

Hybrid Laminar Flow Control (HLFC) systems are employed and a new system is designed and analyzed to show the impact of these systems on an aircraft's efficiency. Hybrid Laminar Flow Control uses a system consisting of ducts and compressors to suck the slowest section of the boundary layer through a carefully designed porous skin at the leading edge of the wing, wingtips or nacelles to suppress instabilities in the airflow and delay the transition to turbulent flow. Since turbulent flow produces up to 10 times more skin friction as laminar flow, HLFC improves the aircraft's performance by reducing the drag, leading to an improved lift/drag ratio which can save fuel, weight or can allow for a larger payload to be carried, all of these factors improve the marketability of the aircraft. The current design is then assessed to determine whether the improvement in performance is worth additional costs associated with the design, installation and running of the system.

A delay on the transition of air over the aircraft surface from laminar to turbulent flow can be achieved by Hybrid Laminar Flow Control technique which has many performance benefits for the aircraft. Before studying laminar flow techniques, the causes of turbulence are reviewed. Transition from laminar to turbulent flow is caused by instabilities in the boundary layer of which there are three main types; Attachment Line Transition (ALT), Crossflow (CF) and Tollmein-Schlichting (TS)[1,2,3].

Laminar flow techniques can be used on wings, engine nacelles, fins and horizontal stabilizers. The benefits of laminar flow control are increased with aircraft size and are maximized for all-wing aircraft[4]. This study focused on techniques relevant to wings but many of the techniques are transferrable onto other parts of the aircraft.

Natural Laminar Flow (NLF) is a passive technique whereby the shape of the wing aerosol is designed to accelerate the flow across the chord of the wing and create a favorable pressure gradient to delay transition due to TS instability amplification. Leading edge radii are sharpened which reduces ReθAL and delays the transition of the attachment line. Typically NLF wings have a low sweep angle and are only usually seen on small to moderately sized aircraft so that the instabilities are predominantly 2D and the effect of surface roughness is reduced. With 2D instabilities only a positive pressure (favorable) gradient is required for them to be suppressed. The airfoil is such that the favorable gradient is maintained as long as possible, often over 50% of the chord. Also there is no leading edge pressure peak because of the reduced leading edge radii[5]. Hybrid Laminar Flow Control was developed combining the advantages of both systems. The airfoil is modified so that the pressure distribution has a favorable pressure gradient for as long as possible and the complex suction system of LFC is limited to the area forward of the front spar which includes all areas of highly 3D instabilities and some of the TS instabilities also; his reduces both the suction requirements and the system complexity. Providing access for maintenance is simplified by using Krueger flaps as the high lift device which when opened provides access to the complete system. The favorable pressure gradient aft of the front spar suppresses the 2D instabilities after the suction region. Active (powered) suction removes the slowest part of the boundary layer which modifies the boundary layer velocity profile in a way that reduces viscous friction[6].

The attachment line is the area of the highest 3D instabilities and therefore requires the highest amount of suction for a given area. By definition the attachment line is at the leading edge where pressure is typically at a maximum; this is approximately at the wing highlight but varies slightly at different flight conditions. Localised areas of passive (unpowered) suction of the attachment line can be achieved by ducting from this region to the low pressure region on the underside of the wing to automatically produce suction[7]. The passive suction region can work in conjunction with the active suction of a HLFC system and is used to ensure that the attachment line is laminar before it enters the active suction region. Here, a HLFC system is designed and investigated which includes regions of passive suction as described above.

II. Air Flow Design

A. Laminar Flow Control

In order to achieve the correct levels of suction at all locations in the suction zone, a fairly complex system is required. Fig. 1 shows a typical HLFC structure and pressure distribution. Although different systems vary, they all contain some form of the following components; a porous skin, skin substructure, collection chambers, pressure restriction control system, ducting, turbocompressor and a power source6. Other considerations which are required in the design stage are high lift devices, anti-ice devices and anti-insect devices. The main aspects are discussed in the following sections.

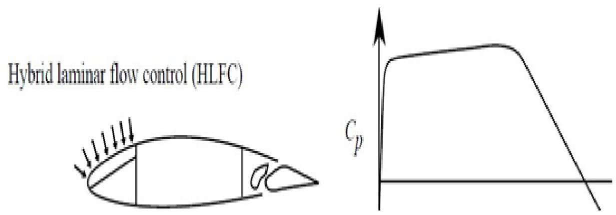

FIGURE 1. Sketch of a typical Hybrid Laminar Flow Control and pressure distribution (1)

The skin defines the external shape of the wing and its careful design can improve the efficiency of the system. Small changes in the shape of the airfoil at the leading edge can have a large impact on the initial pressure gradient which is one of the main parameters in determining the suction requirements. The skin must be made of a suitable material and must be porous to allow air to be sucked through into the collection system. Additional requirements of the skin are that they must be resistant to bird strike and have the ability to maintain their shape and transfer the forces under aerodynamic loading. Furthermore it must have a good surface finish so that transition is not prematurely triggered by any roughness of imperfections.

As a result of these requirements, perforated Titanium is typically used because it has many positive characteristics[8]; it has good erosion resistance and can be surface treated to prevent corrosion so it does not require painting (painting the outer skin is not possible or the perforations would be blocked). It is lighter than Stainless steel and stronger than Aluminum meaning that thinner skins can be used.

Due to unresolved issues regarding the damage detection and repair of carbon fiber, it is not typically used. Composite manufacturers are developing inherently porous material which may become the material of choice in future years as it has the potential to reduce the complexity and weight of the design; the thickness of the material could be varied to control the amount of suction produced along the wings.

A metallic skin must be made porous; this is typically done by drilling an array of holes using either the electron-beam-drilling or laser-drilling techniques. Both techniques produce round, slightly conical holes with a diameter of around 50μm at a rate of 3000 holes per minute. Considering that Billions of holes are required for one wing alone, this is still a long and expensive process.

As shown in Fig. 1, the volume between the outer skin and inner skin is divided by stringers to make spanwise flutes, which guides the air which has been sucked through the porous skin into collectors which are evenly spaced along the suction surface. These stringers also act to strengthen the skin by adding a strong substructure. These flutes lead to collection chambers. Ducts are used to transfer the sucked air from the collection chambers to the turbocompressor. These ducts must be as small as possible to avoid taking up too much valuable space, yet large enough to keep pressure losses low. These ducts merge and lead to a turbocompressor which serves two functions, firstly, to provide the required mass flow rate, and secondly to increase the pressure of the air so that it can be exhausted at the correct pressure (atmospheric pressure).

B. Suction System Design

Initially, the location of the active suction region was determined. As per typical HLFC design, the system would be installed forward of the front spar. For this article, the specimen wing had the front spar at the 15% chord for a majority of the wingspan, this decreased to 10% where there was a kink in the trailing edge of the wing. The spanwise boundaries of the active region is limited by the size of the turbocompressor, therefore the exact sizing of the active suction region was not finalized until later in the analysis, to be optimized for the turbocompressor; the final active system ran from 15.5m to 30m from the aircraft centerline.

The passive suction area is located at airfoil highlight at the inboard end of the active region so that the attachment line Reynold's number is brought below the critical value before entering the active region to reduce the suction/power requirement.

In typical designs, the wing is divided into 3 regions according to the type of instability which is most prevalent in that location. When employing the passive suction device, the ALT active suction is not required and the active suction area is split into two. The crossflow zone is defined as the suction surface in front of the 8% chord line on the upper surface and to the 2% chord on the lower surface where the CF instability is most prevalent, and the Tollmein-Schlichting suction zone is the suction surface aft of the 8% chord line on the upper surface.

It was necessary to choose a wing airfoil which displayed the required pressure characteristics of an HLFC airfoil. Eppler airfoils and NACA 6 and 7 series airfoils were tested using XFOIL and NACA747A315 was found to be best suited for the predicted cruise conditions featuring a rapid initial acceleration so that suppressing the crossflow instability does not require intensive suction.

For an insight analysis and validation, Fluent is hired to evaluate the external pressures acting on the surface of the wing at cruise conditions. Pressure distribution plots were taken at 0.5 m intervals between 15 m and 32 m from the aircraft centerline. There was found to be a favorable pressure gradient up to beyond the 70% chord point when the 3D airfoil was analyzed which will suppress any TS instability aft of the suction region up to this point unless the critical Reynolds number has been exceeded before this. The pressure distribution for the active suction region can be seen in Fig. 2; the plot shows the dramatic increase in pressure at the leading edge. Using these external pressures boundary layer and stability theory calculations are used to determine the suction flow rates required to delay transition[10]. The amount of suction applied is important; if suction is too low, it will not be enough to prevent transition, however if it is too high then the flow into the holes become more three-dimensional and has a higher effective surface roughness which will cause premature transition.

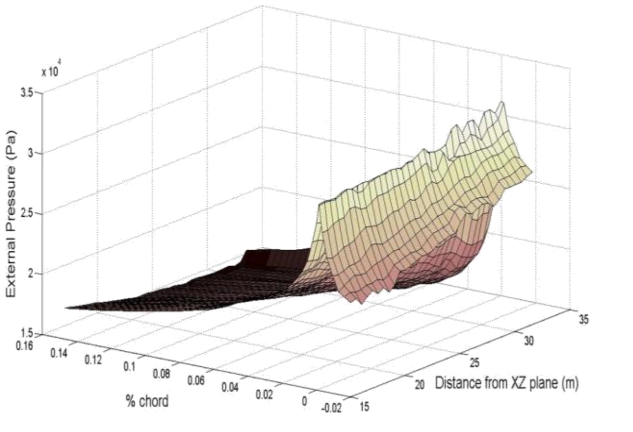

FIGURE 2. External pressure distribution in suction area

C. System analytical investigation

Overall Suction coefficients

Areas of highly 3D instabilities are counteracted by greater local rates of suction therefore the ALT passive suction area and the crossflow area require the most suction. To calculate the level of suction required the suction coefficient, Cq, is first calculated where a higher value of Cq indicates a greater rate of suction. The suction coefficient for each zone is a function of chord length and so must be calculated individually at each spanwise location. The suction surface was divided into 34 spanwise sections of length 0.5 m, and 45 chordwise segments with an approximate length of 0.37% chord. This made a total of 1530 elements with areas proportional to the chord length. The crossflow zone consists of segments 1 to 26 and the Tollmein-Schlichting zone consists of segments 27 to 45. In the following sections the suction coefficients for the different zones are calculated. The passive ALT suction is only required between 15 m and 15.5 m from the aircraft centerline, therefore the calculation has been done for this location and is shown in the following section. The HLFC system is optimised for operation during cruise and so the suction requirements are for the cruise condition.

Anscombe and Illingworth[3] provide equations for calculating the suction coefficient required at the attachment line zone. The attachment line velocity, acting from wing root to tip, is given by:

$$W_{AL} = -0.0032(\Delta P_I)^2 + 1.3048(\Delta P_I) + 38.799 = 85.87 m/s \quad (1)$$

The stream chord Reynolds number, ReC, is calculated as given by:

$$Re_C = \frac{V_{TAS}}{\nu} = 5.19 \times 10^7 \quad (2)$$

where V_{TAS} and ν are true air speed (243.16 m/s) and kinematic viscosity of air (3.7754 x 10-5 m^2/s) respectively, calculated at cruise conditions in a standard atmosphere. c is the chord length (8.05 m). With the sweep angle, Λ, the attachment line momentum thickness Reynolds number can be calculated from:

$$Re_{AL} = \frac{Re_C}{W_{AL}} \sin\Lambda = 489.05 \quad (3)$$

This is far higher than the critical value of 100 so the attachment line will be unstable at this point. Three sub-coefficients (C_{qALA}, C_{qALB}, C_{qALC}) are used to calculate the final attachment line suction coefficient. They are calculated using:

$$C_{qALA} = 64226.75 Re_{\theta AL}^2 = 1.54 \times 10^{10} \quad (4)$$

$$C_{qALB} = -2.8812 Re_{\theta AL} = -1.41 \times 10^3 \quad (5)$$

$$C_{qALC} = 60025(-Re_{\theta AL}^2) = -1.79 \times 10^5 \quad (6)$$

and are combined as follows:

$$C_{qAL} = \frac{C_{qALB} + \sqrt{C_{qALB}^2 - 4C_{qALA}C_{qALC}}}{2C_{qALA}} = 3.4 \times 10^{-3} \quad (7)$$

Anscombe and Illingworth[3] provide further equations for calculating the suction coefficient required at the crossflow zone. Four suction sub-coefficients and the chord Reynolds number are required. The stream chord Reynolds number, Rec, is given by Eq. (2); the sub-coefficients are functions only of the sweep angle and so are the same for all spanwise locations. The sub-coefficients are calculated using Eqs. (8 to 11):

$$C_{qCF1} = (2.687 \times 10^{-13}\Lambda^2) + 6.352 \times 10^{-11}\Lambda - 1.03110^{-9} = 1.86 \times 10^{-9} \quad (8)$$

$$C_{qCF2} = (-6.151 \times 10^{-11}\Lambda^2) + 1.133 \times 10^{-8}\Lambda - 1.385 \times 10^{-7} = 3.97 \times 10^{-7} \quad (9)$$

$$C_{qCF3} = (-2.914 \times 10^{-9}\Lambda^2) + 8.494 \times 10^{-7}\Lambda - 3.96 \times 10^{-6} = 2.47 \times 10^{-5} \quad (10)$$

$$C_{qCF4} = (-1.777 \times 10^{-7}\Lambda^2) + 3.081 \times 10^{-5}\Lambda - 4.972 \times 10^{-4} = 4.34 \times 10^{-4} \quad (11)$$

The overall crossflow suction coefficient is given by:

$$C_{qCF} = C_{qCF1}(Re_C \times 10^{-6})^3 + C_{qCF2}(Re_C \times 10^{-6})^2 + C_{qCF3}Re_C \times 10^{-6} + C_{qCF4} \quad (12)$$

The Tollmein-Schlichting instability is independent of the leading edge geometry and the flight condition. Only a small amount of suction is required and a value of 2 $\times 10^{-4}$ is found to be enough to suppress the 2D instability.

Mass Flow rate

The suction coefficient is linked with volume flow rate as follows:

$$Q = C_q V_\infty S \quad (13)$$

where S is the surface area of the suction surface (m^2) and V_∞ is the freestream velocity (m/s). C_q refers to the local suction coefficient. Furthermore, by multiplying by the air density, the mass air flow through the surface could be calculated for each element.

The variation in volume flow rate for the active suction zones can be seen in Fig. 3. Since the volume flow rate is a function of suction area and C_q and both of these are factors of the chord length the flow rate required is less when closer to the wing tip. The flow rate required has been ramped up to the calculated value rather than an instant change. This is in case a sudden change in the amount of suction induces turbulence rather than suppressing it.

The suction surface was designed as a corrugated fiberglass skin substructure bonded to a perforated titanium outer skin. The fiberglass substructure is lightweight but rigid enough to transfer the flight loads and allows for an electric blanket anti-icing system to be used. Regarding anti-insect devices, an anti-insect spray will be installed in the Krueger flap which when coupled with the flap acting as a deflector provides sufficient protection against insect debris.

The perforated skin will be drilled from the inside surface to eliminate the problem of insects or dust being lodged in the holes and to avoid any undesirable effect, the holes will be drilled perpendicularly to the surface. To give a reasonable compromise between flute size and substructure strength, a flute width of 7.5 mm has been used near the leading edge where higher impact strength is required; the width is 15 mm when away from this area. A schematic is shown in Fig. 4. The width of the stringer will be the same as the flute width to give the heat from the electric blanket as much area to conduct through without blocking too much of the suction space. With this substructure design, the effective suction area is halved, therefore the suction coefficient values must be doubled in the remaining suction area so that the required volume flow rate is maintained[9].

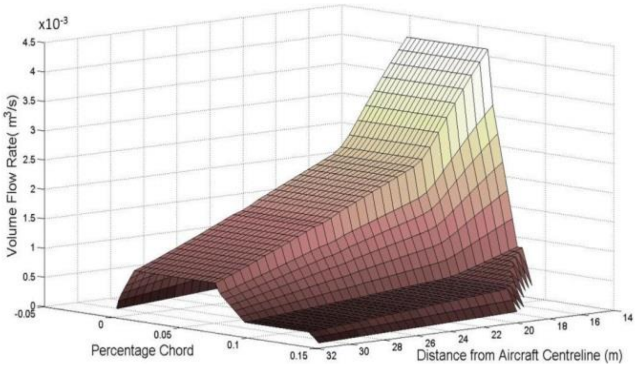

FIGURE 3. Volume flow rate required for active suction

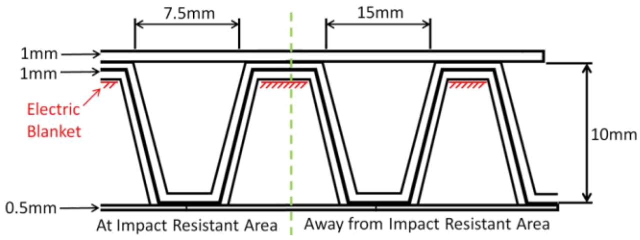

FIGURE 4. Skin and substructure design

Perforated Surface Optimization

The perforated skin is the boundary between the external pressure, defined by both nature and the flight condition, and the flute's internal pressure. The internal pressures along the flutes can be determined by design; by sizing the turbocompressor and the ducting to set the internal pressure in the collectors as required. It is essential that the pressure drop across the porous skin is the same as the pressure drop needed to achieve the required level of suction calculated in the previous section. The sizing and spacing of the holes in the perforated skin can be varied to ensure that this pressure drop is achieved. In order to do this it is necessary to understand the link between the perforation geometry and spacing, and the resulting pressure drop across the skin. The equations used for this are given in the following section.

It is also necessary to know how the pressure inside the flutes varies between the collectors of known pressure. For the design of the perforated skin in this article it has been assumed that the pressure within the flutes varies linearly between collectors; any errors in this assumption will not affect the system architecture and can be resolved by re-optimizing the hole configuration once a more accurate understanding of the between-collector pressure drop is understood.

The design of a perforated surface has limitations. Firstly, current hole-drilling technologies (laser-drilling or electron-beam drilling) are limited to a minimum hole diameter of 50 μm in a 1 mm sheet of titanium. Secondly, to maintain the structural integrity of the skin, the spacing ratio of the perforations must be greater than five. Finally, the maximum hole velocity, V_H, is limited to 40 m/s; a velocity greater than 50 m/s will result in premature transition because the effective roughness would be too high, 40 m/s is a safer limit10. V_H, can be calculated using:

$$V_H = \frac{V_S}{G} \quad (14)$$

where G is the porosity of the perforated surface defined as:

$$G = \frac{\pi}{4N^2} \quad (15)$$

where N is the spacing ratio; the ratio of the distance between holes from center to center (m) and the hole diameter, d (m).

With V_H and the hole geometry determined, the mass flow rate of air through an individual hole, $\dot{m}$, (kg/s) can be calculated using:

$$\dot{m} = \rho V_H A \quad (16)$$

where ρ is the density of the air (kg/m^3) and A is the hole area (m^2).

The pressure drop, Δp, (Pa) across the skin is then calculated using:

$$\Delta p = \frac{Y \rho v^2 t^2}{d^4} \quad (17)$$

where v is the kinematic viscosity of air (m^2/s), t is the skin thickness and Y is given by:

$$Y = \frac{1}{K_d}(40.7X + 1.95X^2) \quad (18)$$

where K_d is the ratio between the effective hole diameter and the measured hole diameter which for laser-drilled holes is stated as 1.3 (Ref. 6). X is found using:

$$X = \frac{\dot{m}}{\mu t} \quad (19)$$

where μ is the dynamic viscosity of air (kg/m s). The aim of optimizing the perforated surface is to vary the hole spacing to achieve the required pressure drop whilst ensuring the hole air velocity and hole spacing limits are not exceeded.

D. Validation of Suction Region Design

Computational Fluid Dynamics (CFD) software is applied to perform the numerical simulation as a process of validation of suction region design. Different models were run with the porosity of the porous section varied. An example of the typical results is shown in Fig. 5 indicates the variation in velocity at the leading edge of the airfoil. It can also be seen that at the leading edge, due to the suction there is also a reduction of pressure at the suction region relative to the porosity of the suction surface and the areas outside of the suction region (from 0.2% chord) are at a slightly higher pressure as a result. The reduction of pressure at the inlet is very small compared to the reduction at the exhaust. This means that the overall pressure drop between the inlet and exhaust has increased by approximately 3500 Pa which will induce more suction than required and may result in VH exceeding the limit of 40 m/s.

This shows that the design of the passive suction surface must be an iterative process; the steps previously presented in would be the first iteration after which the inlet and exhaust pressures must be input back into the initial calculations to converge upon a suitable value of porosity. Alternatively, a control valve within the duct could be used to ensure that the maximum mass flow rate is not exceeded.

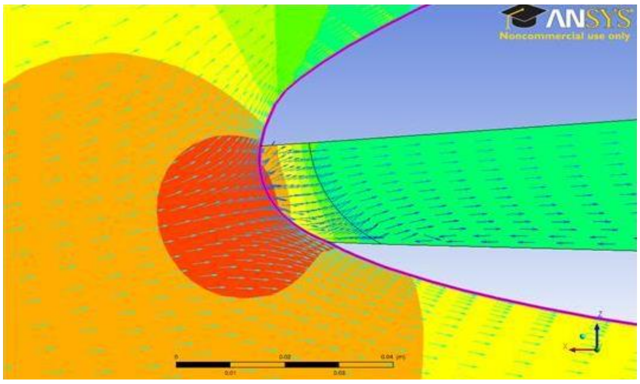

FIGURE 5. Velocity contour at leading edge

III. PERFORMANCE ANALYSIS

A. Drag Calculation

The benefit of the HLFC system is that the friction drag over the wing is reduced by around 90%. This means a better fuel consumption so less fuel is required for the same mission. The disadvantage of the system is that it adds additional weight to the aircraft. This section details the calculations for determining whether the benefit of the system outweighs the disadvantages by first calculating the drag saving using a technique described by Sadraey[11], then estimating the system mass and finally performing a weight penalty analysis for the overall system for the design mission.

Outer Wing Drag without HLFC

The typical aircraft wing drag polar contains both a lift dependent coefficient, K, and a non-lift dependent coefficient, C_{Do}, also known as the zero-lift drag coefficient:

$$C_D = C_{Do} + KC_L^2 \quad (20)$$

The HLFC system only improves the skin friction drag which is contained within C_{Do} so it is only necessary for this value to be analyzed. This value can be calculated using:

$$C_{Do} = C_{fw}\, f_{tc}\, f_M \left(\frac{S_{wet}}{S}\right)\left(\frac{C_{Dmin}}{0.004}\right)^{0.4} \quad (21)$$

C_{fw} varies depending on whether the flow around the wing is laminar or turbulent. As mentioned previously, because of the high sweep angle the whole outer wing will be in turbulent air because the attachment line will be unstable. Therefore the equation for C_{fw} is:

$$C_{fw(turb)} = \frac{0.455}{[\log_{10}(Re_C)]^{2.58}} \quad (22) \qquad (22)$$

where Re_c is the chord Reynolds number. Rec for each 0.5 m span section was previously calculated. The parameter f_{tc}, is a function of the thickness ratio of the wing and is given by:

$$f_{tc} = 1 + 2.7\left(\frac{t}{c}\right)_{max} + 100\left(\frac{t}{c}\right)^4_{max} \quad (23)$$

where t is the maximum thickness and C is the chord. For the outer wing the thickness ratio is 10% and therefore f_{tc}=1.28. The parameter f_M is a function of Mach number, M, and is defined as:

$$f_M = 1 - 0.08M^{1.45} \quad (24)$$

which for the design cruise speed of M=0.82 is calculated as 0.94.

S_{wet} is the wetted area of the outer wing and S is the net area. These are calculated by taking measurements from a 3D model to be 128.151 m^2 and 62.922 m^2 respectively. C_{dmin} is the minimum drag coefficient of the wing airfoil and is read directly from the C_d/C_L curve of the NACA747A315 airfoil as 0.01716.

With this information, C_{Do} was calculated for each span section which was converted into drag (N) using:

$$d = 0.5C_{Do}\,\rho\,V_{TAS}^2\,S \quad (25)$$

where S is the net area for each span segment. The total drag of the outer wing in the area where HLFC is active is 7886 N.

Outer Wing Drag with HLFC

To calculate the drag of the outer wing when the HLFC system is being used is it is first necessary to predict where transition will occur on the wing and then calculate the total drag as before but with an alternate value of C_{fw} in the laminar areas.

The extent of the laminar flow when a HLFC system is used is limited by the smaller of two factors; firstly the location of the start of the adverse pressure gradient and secondly the Reynolds number at which transition occurs. The former limit is at a fixed percentage chord and occurs at the outbound regions of the wing where the chord is smaller; using CFD, the adverse pressure region shown to approximately start at the 73% chord. The latter limit occurs at more inboard regions with a larger chord where the maximum physical distance is reached before the adverse pressure region begins. The Reynolds number limit is represented by a line parallel to the leading edge which corresponds to a critical transition Reynolds number, Re_{tran}; taken as 25x106 (Ref. 2). The distance is calculated using:

$$X = \frac{Re_{tran}\,\nu}{V_{TAS}} = \frac{25\times10^6\times3.775\times10^{-5}}{243.2} = 3.88\text{ m}$$

(26)

Figure 6 shows the extent of both laminar limits and hence the laminar flow region.

C_{fw} for areas of laminar flow for each spanwise section were calculated using:

$$C_{fw(lam)} = \frac{1.327}{\sqrt{Re_C}} \quad (27)$$

C_{Do} was recalculated for each spanwise section where the value of C_{fw} used was calculated based on the proportion of the wing section area in laminar flow using the equation:

$$C_{fw} = C_{fw(lam)}\left(\frac{S_{lam}}{S_{turb}}\right) + C_{fw(turb)}\left(1 - \left(\frac{S_{lam}}{S_{turb}}\right)\right)$$

(28)

where Slam and Sturb are the areas of the wing section in laminar and turbulent flow respectively. Note that the whole underside of the wing is assumed to be turbulent so the under-wing area must be included in Sturb. New value of drag. This gives a zero-lift drag for one outer wing of 5710 N, a 27.6% reduction. The variation of drag across the outer wing can be seen in Figure 7.

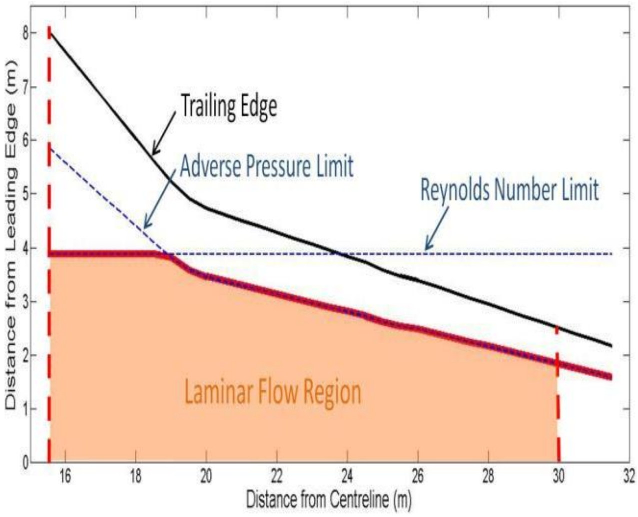

FIGURE 6. Laminar Flow Limit

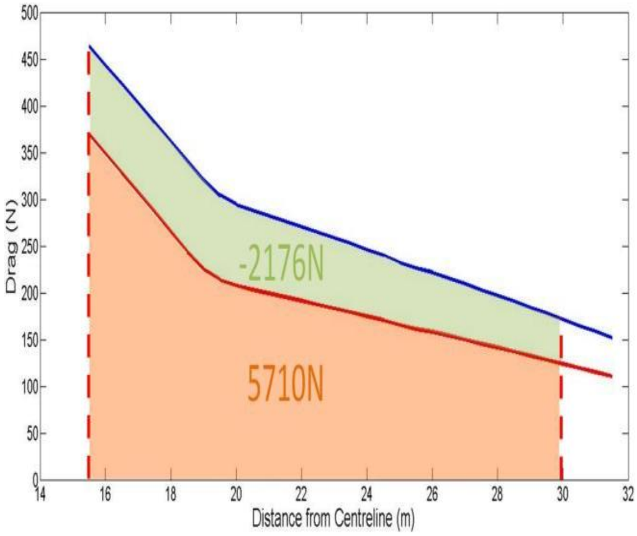

FIGURE 7. Drag saving due to HLFC

B. System Weight Penalty

The system is analyzed to determine if this drag saving is beneficial as the weight of the system and the power required to run the system reduce the efficiency of the aircraft. The integration of the HLFC system into both wings of the candidate aircraft was estimated to produce an increase in weight of 490kg. The system weight penalty, WT, is the weight of the system (WA) plus the fuel penalties. The fuel penalty is the additional weight of the fuel due to system effects. This is due to three factors; the weight of the system ($\Delta W_{fo(\Delta WA)}$), the reduction in engine performance due to the additional power off-take requirements of the system ($\Delta W_{fo(\Delta fp)}$), and the increase in aircraft drag due to the system ($\Delta W_{fo\Delta d}$). For the latter factor, HLFC systems are unique in that there is a decrease in drag making the value of $\Delta W_{fo\Delta d}$ negative. The system weight penalty is given by:

$$W_T = \Delta W_A + \Delta W_{fo(\Delta W_A)} + \Delta W_{fo(\Delta fp)} + \Delta W_{fo(\Delta d)}$$
(29)

It is assumed that for a given mission, the aircraft travels at cruise conditions at an average aircraft mass taken with 60% of the design fuel. This assumption is close enough to reality because the increase in fuel consumption on the climb segment is balanced by the reduction in fuel consumption in the descent segment.

Both the zero-redundancy and the double-redundancy system were analyzed. The mass of both systems were calculated in the previous section and therefore W_A is 4804.4N and 6148.4 N respectively.

$\Delta W_{fo(\Delta WA)}$ can be calculated using:

$$\Delta W_{fo(\Delta W_A)} = \Delta W_A\left(e^{(sfc)tg/r} - 1\right) \qquad (30)$$

where sfc is the SFC of the engine at cruise conditions (kg/Ns), t is the time taken for the mission, g is the acceleration due to gravity and r is the average lift/drag ratio at cruise which for the aircraft was found to be 18. To calculate the SFC at cruise conditions, a virtual engine model was developed using TURBOMATCH[12] software that allows the user to build a model of the engine using blocks with variable properties to simulate an engine's performance. Using the virtual model, the SFC was found to be 14.71x10-6 kg/Ns. The mission time is estimated by dividing the mission range (7500 nm) by the true airspeed at cruise; this gives a time of approximately 57000 s. Therefore $W_{fo(\Delta Wa)}$ is 2790.6 N for the zero redundancy architecture and 3571.2 N for the double redundancy architecture.

To determine the reduction in aircraft engine performance (and therefore $W_{fo(\Delta fp)}$ it was necessary to calculate the offtake power required from the engines to power the turbocompressors. Turbocompressors within the HLFC system serve two functions, firstly, to provide the required mass flow rate, and secondly to increase the pressure of the air so that it can be exhausted at the correct pressure (atmospheric pressure). The power, P, in Watts required for a turbocompressor can be found using:

$$P = \frac{\Delta p\, Q}{\eta} \qquad (31)$$

where Δp is the difference in pressure across the turbocompressor (Pa), η is efficiency and Q is the volume flow rate of air normalized to sea level conditions (m3/s). Normalized volume flow rate is calculated by dividing the flow rate at cruise conditions and dividing this by the ratio of density at sea level to density at cruise conditions. Using Eq. (37) and assuming a turbocompressor efficiency of 0.8 and a motor efficiency of 0.95, the maximum power required per wing for the turbocompressor is 7.26 kW.

$\Delta W_{fo(\Delta fp)}$ can be calculated using:

$$\Delta W_{fo(\Delta fp)} = \frac{r\Delta f_p}{sfc}\left(e^{(sfc)tg/r} - 1\right) \qquad (32)$$

where Δf_p is the rate of fuel used due to the power off-take required for the turbocompressors. sfc, t, g and r are as before. Δf_p can be calculated using:

$$\Delta f_p = \Delta(sfc) \times T_{NET} \qquad (33)$$

where Δ(sfc) is the increase in engine SFC due to the system, and TNET is the net thrust for cruise. The net thrust at cruise for the aircraft is 84 kN and the increase in SFC was found to be 1.3772x10-9 kg/Ns by running a TURBOMATCH simulation of the engine in cruise and increasing the off-take by 7.26 kW (i.e. the power required per wing for the HLFC system). Therefore Δf_p is calculated as 11569 kg/s and Wfo(Δfp) is 82.2 N.

In the HLFC system the drag reduction must be subtracted from the ram drag to get the total change in drag.

From previous calculations, the mass flow rate of air taken in by the system is 1.015 kg/s. The ram drag can be calculated as follows:

$$d_{ram} = m \times V_{TAS} = 1.01\dot{5} \times 243 = 246.8N \quad (34)$$

As previously calculated, the drag saving per wing is 2176 N so the overall change in drag is given by:

$$\Delta d = d_{ram} - 2d_{wing\ saving} = 24\dot{6} - (2 \times 2176) = -4106N \quad (35)$$

With all parameters W_T can be used to calculate as:

$$W_T = 6148.4 + 2790.6 + 82.2 - 42926 = -35248.8N \quad (36)$$

The fact that W_T is both large and negative shows that the advantage of the drag reduction significantly surpasses the disadvantages of the system weight and fuel penalty. This results in a mass saving of 3593.1 kg . The total weight of fuel saved for the 7500 nm mission can be calculated using:

$$\Delta W_{fo} = \Delta W_{fo(\Delta Wa)} + \Delta W_{fo(\Delta fp)} + \Delta W_{fo(\Delta d)} \quad (37)$$

which gives a weight saving of 40053 N (i.e. 4083 kg).

IV. Conclusion

The hybrid laminar flow system utilizes both active and passive suction and fulfils the requirement of improving the aircraft performance. The active suction suppresses the crossflow and Tollmein-Schlichting instabilities from just below the leading edge highlight to the front spar. The passive suction automatically sucks the attachment line boundary layer to delay the attachment line transition which is essential for the active suction to be as effective.

Overall, it is advantageous to incorporate the HLFC system into the aircraft because the over 3500 kg can be saved. This means that either the payload could be increased by 12% which makes the aircraft significantly more profitable. Alternatively, 3500 kg of extra fuel would increase the aircraft range by 5%. This makes the aircraft more marketable; particularly as more fuel efficient aircraft are becoming more of a priority as fuel prices continue to increase.

The anti-insect device consists of the Krueger flap which acts as a deflector, and an anti-insect spray mounted on the Krueger flap directed at the leading edge. The turbocompressors are electrically powered.

In the current design only 50% of the overall suction area is used for suction, the other 50% is taken up by the wide stringers required for the anti-icing system; however with a more solid substructure the stringer thickness could be reduced so there is more suction area. This would mean that for there are more holes for the air to flow through which means that the requirement for VH to be less than 40 m/s would be easier to achieve allowing more flexibility in the porous surface design which may mean that each collector may not need to be split into as many sections and the part count could be reduced.

The design could achieve a drastic gain of a fuel weight saving of 40053 N or 4083 kg.

It is recommended a further work to be done by changing the location of turbocompressors to the near the engines so bleed air can be ducted directly into the ducts to clear any dust or insects that may have clogged any holes in the porous skin (although careful design of the skin has minimized this likelihood). Any water in the ducts (either from rain, mist or melted ice) will be evaporated by the hot bleed air and will be exhausted out of the porous skin at the same time. The engine has been designed to be able to cope with the required amount of bleed air offtake.

References

[1]Joslin, R.D, “Overview of Laminar Flow Control,” NASA/TP-1998-208705, 1998.

[2]Naranoot, W, “A Design Study of Long Range Subsonic Transport Aircraft Using Hybrid Laminar Flow Control on the Wing,” MSc. Thesis, School of Engineering, Cranfield Univ., Bedfordshire, UK, 1999.

[3]Anscombe, A., and Illingworth, L.N., “Wind Tunnel Observations of Boundary Layer Transition on a Wing at Various Angles of Sweepback,” Aeronautical Research Council, 1956.

[4]Lachmann, G.V., “Aspects of Design Engineering and Operational Economy of Low Drag Aircraft.,” *Boundary Layer and Flow Control,* Vol. 2, 1961, pp. 1123-1166.

[5]Wilson, R.A.L., “The Introduction of Laminar Flow to the Design and Optimisation of Transport Aircraft,” Ph.D. Dissertation,, School of Engineering, Cranfield Univ., Bedfordshire, UK, 1997.

[6]Wood, A., “Design Study on the Use of Distributed Pumping Within a Hybrid Laminar Flow Control System,” MSc. Thesis, School of Engineering, Cranfield Univ., Bedfordshire, UK, 2003.

[7]NASA, “High Reynolds Number Hybrid Laminar Flow Control (HLFC) Flight Experiment II. *Aerodynamic Design*,” NASA/CR-1999-209326, 1999.

[8]Thomas-Bourgneuf, V., “Numerical Modelling and Analysis of a Novel Hybrid Laminar Flow System,” MSc. Thesis, School of Engineering, Cranfield Univ., Bedfordshire, UK, 2010.

[9]NASA, “High Reynolds Number Hybrid Laminar Flow Control (HLFC) Flight Experiment IV. *Suction System Design and Manufacture*,” NASA/CR-1999-209326, 1999.

[10]Stellars, N.D., “A Study to Indicate the Number of Plenum Chambers Required for a HLFC System on a Military Delta Wing/Canard Configurations,” Bae-BAE-RP-RES-5510, 1999 (unpublished).

[11]Sadraey, M., “Aircraft Performance Analysis,” VDM Verlag Dr. Müller, 2009.

[12] TUBRBOMATCH, a tool for aero-engine modelling and management, Cranfield University, UK